PHYSICAL REVIEW E **79**, 010901(R) (2009)

Spontaneous calcium signals induced by gap junctions in a network model of astrocytes

V. B. Kazantsev*

Institute of Applied Physics of Russian Academy of Science, 46 Uljanov Strasse, 603950 Nizhny Novgorod, Russia and Department of Neurodynamics and Neurobiology, Nizhny Novgorod State University, 23 Gagarin Avenue, 603950 Nizhny Novgorod, Russia

(Received 25 February 2008; revised manuscript received 10 October 2008; published 14 January 2009)

The dynamics of a network model of astrocytes coupled by gap junctions is investigated. Calcium dynamics of the single cell is described by the biophysical model comprising the set of three nonlinear differential equations. Intercellular dynamics is provided by the diffusion of inositol 1,4,5-trisphosphate (IP_3) through gap junctions between neighboring astrocytes. It is found that the diffusion induces the appearance of spontaneous activity patterns in the network. Stability of the network steady state is analyzed. It is proved that the increase of the diffusion coefficient above a certain critical value yields the generation of low-amplitude subthreshold oscillatory signals in a certain frequency range. It is shown that such spontaneous oscillations can facilitate calcium pulse generation and provide a certain time scale in astrocyte signaling.

DOI: 10.1103/PhysRevE.79.010901 PACS number(s): 87.18.Hf, 82.40.Bj, 05.45.−a, 89.75.Kd

Recent experimental findings have shown that calcium signals in astrocytes may play an important role by regulating cellular functions and information transmission in the nervous system [1–7]. In contrast with neuronal cells the astrocytes do not generate electrical excitations (action potentials). However, their intracellular dynamics have shown similar excitable properties for changes of calcium concentration [4]. These signals can remarkably affect neuronal excitability and the efficiency of synaptic transmission between neurons by Ca^{2+}-dependent release of neuroactive chemicals (e.g., glutamate or ATP). Networks of astrocytes accompanying neuronal cells generate collective activity patterns that can regulate neuronal signaling by facilitating or by suppressing synaptic transmission [4–6]. For example, such patterns can be treated as "templates" guiding information along different transmission pathways in a neuronal system [7].

In a number of previous studies a biophysical mechanism underlying calcium dynamics has been extensively investigated [8–12]. Calcium is released from internal stores, mostly from the endoplasmic reticulum (ER). This process is regulated by inositol 1,4,5-trisphosphate (IP_3) that activates IP_3 channels in the ER membrane resulting in a Ca^{2+} influx from ER. IP_3 acting as a second messenger is produced when neurotransmitters (e.g., glutamate or ATP) are bound by metabotropic receptors of the astrocyte. In turn IP_3 can be regenerated depending on the level of calcium by the phospholipaise C-δ (PLC-δ). Intercellular communication between astrocytes is provided by two basic mechanisms comprising the diffusion of intracellular IP_3 via gap junctions and extracellular diffusion of ATP released by the astrocytes [9]. Depending on the brain area these mechanisms contribute differently to the astrocyte connectivity. Here we will focus on gap junction coupling. In astrocytes these junctions are built with Cx43 mostly permeable to IP_3 which can propagate at a relatively long distance (up to 300 μm) [9]. Previous papers have discussed a number of interesting nonlinear phenomena found in astrocytes including glutamate induced oscillations in an isolated cell [8], modulation and information encoding by calcium signals [10], phase synchrony of oscillations due to the IP_3 diffusion [11], IP_3 and ATP induced wave propagation [12], neuron-glial interaction and its possible regulatory role in information processing [2–6], and many others.

This Rapid Communication reports on a mechanism of spontaneous calcium signaling and pattern formation in an astrocyte network induced by IP_3 diffusion through gap junctions. We will show that there exists a critical value of the diffusion coefficient above which originally nonoscillating cells due to the diffusion start to generate spontaneous subthreshold oscillations. Such dynamics is not typical for most of the reaction-diffusion networks where the diffusion normally tends to homogenize the diffusing component, hence stabilizing the homogeneous distribution or synchronizing network in case of oscillatory kinetics (neuronal oscillators, cardiac cells, etc.).

Let us consider a mathematical model of the astrocyte network in the form of a two-dimensional square lattice with only nearest-neighbor connections [11]. Such topology for the IP_3-diffusion model is justified by recent experimental findings stating that astrocytes occupy "nonoverlapping" territories [13]. State variables of each cell include IP_3 concentration, $p_{j,k}=[IP_3]$, Ca^{2+} concentration, $[Ca^{2+}]=z_{j,k}$, and the fraction of activated IP_3 receptors, $q_{j,k}$. They evolve according to the following equations:

$$\dot{p}_{j,k} = P(p_{j,k}, z_{j,k}, q_{j,k}) + k_{IP_3}(\Delta p)_{j,k},$$

$$\dot{z}_{j,k} = Q(p_{j,k}, z_{j,k}, q_{j,k}),$$

$$\dot{q}_{j,k} = R(p_{j,k}, z_{j,k}, q_{j,k}), \tag{1}$$

with $j,k=1,2,\ldots,N$. $(\Delta p)_{j,k}=(p_{j+1,k}+p_{j-1,k}+p_{j,k+1}+p_{j,k-1}-4p_{j,k})$ is a discrete Laplace operator. We imply zero-flux (Neumann) boundary conditions, $p_{0,k}=p_{1,k}$, $p_{j,0}=p_{j,1}$, $p_{N+1,k}=p_{N,k}$, $p_{j,N+1}=p_{j,N}$. Parameter k_{IP_3} describes the IP_3 diffusion rate. Nonlinear functions P,Q,R defining local cell dynamics can be expressed as follows [8,11]:

*vkazan@neuron.appl.sci-nnov.ru

 ©2009 The American Physical Society

$$P(p,z,q) = (p^* - p)/\tau_{IP_3} + J_{PLC},$$

$$Q(p,z,q) = J_{chan} - J_{pump} + J_{leak} + J_{in} - J_{out},$$

$$R(p,z,q) = a_2\left(d_2\frac{p+d_1}{p+d_3}(1-q) - zq\right). \quad (2)$$

Here $J_{PLC}=v_4[z+(1-\alpha)k_4]/(z+k_4)$ is the calcium-dependent PLC-δ current, p^* is the steady-state concentration of IP_3, τ_{IP_3} is the relaxation constant, $J_{chan}=c_1v_1p^3z^3q^3[\frac{c_0}{c_1}-(1+\frac{1}{c_1})z]/[(p+d_1)(z+d_5)]^3$ is Ca^{2+} current from ER to cytosol, $J_{pump}=v_3z^2/(k_3^2+z^2)$ is the ATP pumping current, $J_{leak}=c_1v_1[\frac{c_0}{c_1}-(1+\frac{1}{c_1})z]$ is the leak current, currents $J_{in}=v_5+v_6z^2/(k_2^2+z^2)$ and $J_{out}=k_1z$ describe calcium exchanges with extracellular space. Biophysical meaning of all parameters in Eqs. (2) and their values determined experimentally can be found in [8,11]. For our purpose we fix $c_0=2.0$ μM, $c_1=0.185$, $v_1=6$ s^{-1}, $v_2=0.11$ s^{-1}, $v_3=2.2$ μM s^{-1}, $v_5=0.025$ μM s^{-1}, $v_6=0.2$ μM s^{-1}, $k_1=0.5$ s^{-1}, $k_2=1.0$ μM, $k_3=1.0$ μM, $a_2=0.14$ μM^{-1} s^{-1}, $d_1=0.13$ μM, $d_2=1.049$ μM, $d_3=0.9434$ μM, $d_5=0.082$ μM, $\alpha=0.7$, $\tau_{IP_3}=7.143$ s, $p^*=0.16$ μM, $k_4=1.1$ μM and take the rate of IP_3 regeneration, $v_4\sim 0.3-2$ μM s^{-1} and IP_3 diffusion coefficient, $k_{IP_3}\sim 0.01-1$ s^{-1} as control parameters.

The dynamics of isolated cell [$k_{IP_3}=0$ in Eqs. (1)] has been studied in detail in [11]. For $v_4<v_4^{AH}\approx 0.3809$ μM s^{-1} there exists stable fixed point $O(p_0,z_0,q_0)$ (of node or focus type) in the phase space. It defines stable equilibrium concentrations of IP_3 and Ca^{2+}. This fixed point loses its stability via supercritical Andronov-Hopf bifurcation at $v_4=v_4^{AH}$ and a stable limit cycle appears. It corresponds to the intracellular calcium oscillations of about 0.05–0.1 Hz frequency and 0.5 μM amplitude.

Let us consider the dynamics of astrocytes (1) exchanging IP_3 via the gap junctions. We assume that $v_4<v_{AH}$, hence each local cell exhibits stable equilibrium calcium concentration. It is associated with homogeneous steady state $O(p_{j,k}=p_0,z_{j,k}=z_0,q_{j,k}=q_0)$. Linearizing Eqs. (1) near this state one can write the linear $3N$-dimensional system for local perturbations. Expressing these perturbations in the exponential form, $p_{j,k}=A_{j,k}\exp\lambda t$, $z_{j,k}=B_{j,k}\exp\lambda t$, $q_{j,k}=C_{j,k}\exp\lambda t$, we obtain an algebraic linear system for the amplitudes $A_{j,k}$, $B_{j,k}$, $C_{j,k}$. By excluding $B_{j,k}$ and $C_{j,k}$ we find

$$SA_{j,k} + A_{j+1,k} + A_{j-1,k} + A_{j,k+1} + A_{j,k-1} = 0,$$

$$j,k = 1,2,\ldots,N, \quad (3)$$

with

$$Sk_{IP_3} = P_p - 4k_{IP_3} - \lambda + \frac{P_z(-\lambda Q_p + Q_pR_q - Q_qR_p)}{Q_qR_z - (R_q-\lambda)(Q_z-\lambda)}, \quad (4)$$

and with the zero-flux boundary conditions. Constants $P_{p,z,q}$, $Q_{p,z,q}$, $R_{p,z,q}$ in Eq. (4) denote partial derivatives of functions (2) taken in the steady-state O. Substituting $A_{j,k}=u_jv_k$ in Eqs. (3) and separating the variables we find that Eqs. (3) are equivalent to the following equations [14]:

$$(S-\rho)u_j + u_{j-1} + u_{j+1} = 0,$$

$$\rho v_k + v_{k-1} + v_{k+1} = 0,$$

$$u_0 = u_1, \quad u_{N+1} = u_N, \quad v_0 = v_1, \quad v_{N+1} = v_N, \quad (5)$$

where ρ is a free parameter. Characteristic determinants, $D_N^{(1)}$, $D_N^{(2)}$, for linear homogeneous equations (5) can be expressed as follows:

$$D_N^{(1)}(S,\rho) = (S-\rho+2)U_{N-1}[(S-\rho)/2] = 0,$$

$$D_N^{(2)}(\rho) = (\rho+2)U_{N-1}(\rho/2) = 0, \quad (6)$$

respectively, where $U_m(x)$ is Chebyshev polynomials. Finding their roots, $x=\cos s\pi/(m+1), s=1,2,\ldots,m$ and excluding free parameter ρ we obtain

$$S = 2\left(\cos\frac{s\pi}{N} + \cos\frac{l\pi}{N}\right),$$

$$s,l = 1,2,\ldots,N. \quad (7)$$

Substituting S to (4) we find that the spectrum of $3N$ eigenvalues of the steady state is defined by the following characteristic equation:

$$\lambda_{s,l}^3 - \lambda_{s,l}^2(\tilde{P}_p + Q_z + R_q) + \lambda_{s,l}(Q_zR_q - Q_qR_z + \tilde{P}_pR_q + \tilde{P}_pQ_z - P_zQ_p) + (\tilde{P}_pQ_qR_z - \tilde{P}_pR_qQ_z + P_zQ_pR_h - P_zQ_hR_p) = 0, \quad (8)$$

with

$$\tilde{P}_p = P_p - 4k_{IP_3} - 2k_{IP_3}\left(\cos\frac{s\pi}{N} + \cos\frac{l\pi}{N}\right),$$

$$s,l = 1,2,\ldots,N.$$

Solving Eq. (8) we find that with increasing k_{IP_3} pairs of eigenvalues with positive real parts sequentially appears in the spectrum. The dependence of the largest exponent $\lambda_{max}=\max_{s,l}\mathrm{Re}\,\lambda_{sl}$ on k_{IP_3} is illustrated in Fig. 1(a). For $k_{IP_3}=k_{IP_3}^*$ a pair of complex conjugate eigenvalues crosses the imaginary axis. It corresponds to Andronov-Hopf bifurcation in the $3N$-dimensional phase space when the steady state loses its stability and the stable limit cycle appears. This limit cycle defines spontaneous oscillations involving all units of the network with frequency that can be estimated by the imaginary part of the eigenvalues.

With further increase of k_{IP_3} next pairs of complex conjugate eigenvalues sequentially get positive real parts leading to a multifrequency oscillation pattern. Note that corresponding bifurcation values of k_{IP_3} come very close to each other for large N. The range of unstable "eigenfrequencies" $f_{sl}\approx\mathrm{Im}\,\lambda_{sl}/2\pi$ depending on k_{IP_3} is illustrated in Fig. 1(b). It appears that the oscillatory eigenmodes (e.g., oscillations at eigenfrequencies) are localized near 0.11 Hz in a quite narrow band extended with growing k_{IP_3}.

In the linear limit the general solution of the network would be a linear superposition of oscillations at the eigenfrequencies. In the case of nonlinear equations (1) the solution will be the result of a nonlinear interaction of these

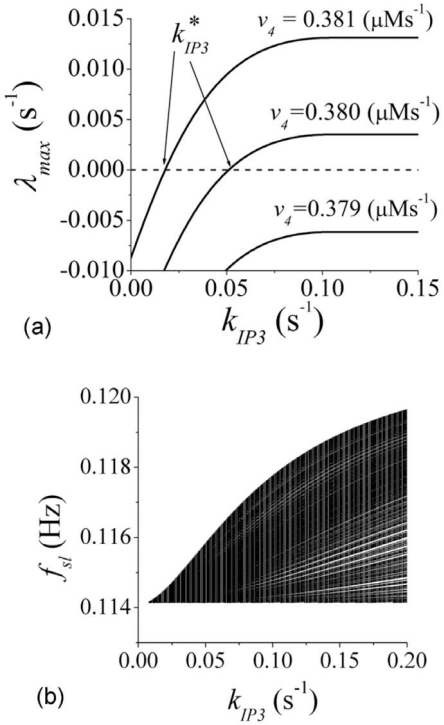

FIG. 1. (a) The dependence of the largest steady-state eigenvalue on k_{IP_3} for different v_4. (b) Eigenfrequencies $f_{sl}=\mathrm{Im}\,\lambda_{sl}/2\pi$ are the corresponding unstable eigenmodes. Parameters, $v_4=0.3805\ \mu\mathrm{M\ s^{-1}}$, $N=30$.

eigenmodes. For the low amplitude oscillations such interaction will be weak and can be treated in terms of Taylor expansion of the nonlinear functions (2) up to the cubic terms providing the saturation of the oscillation growth. At the same time one can expect composite frequencies in the Fourier spectrum and, hence, slow modulation of the amplitude at difference frequencies appears due to the quadratic terms, $\Delta f \sim f_n - f_m$, where f_n and f_m are the eigenfrequencies taken from the unstable branch. Indeed, Fig. 2 shows such modulation in the profiles of the oscillatory signals emerging from the instability.

In the plane of control parameters (v_4, k_{IP_3}) the instability region is located above the curve $k^*_{IP_3}(v_4)$ shown in Fig. 3.

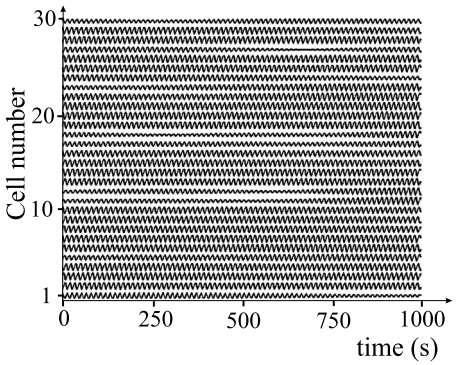

FIG. 2. Raster plot of subthreshold calcium signals, z_{jk}, taken from the row at $k=15$, $v_4=0.3805\ \mu\mathrm{M\ s^{-1}}$, $k_{IP_3}=0.02\ \mathrm{s^{-1}}$, $N=30$.

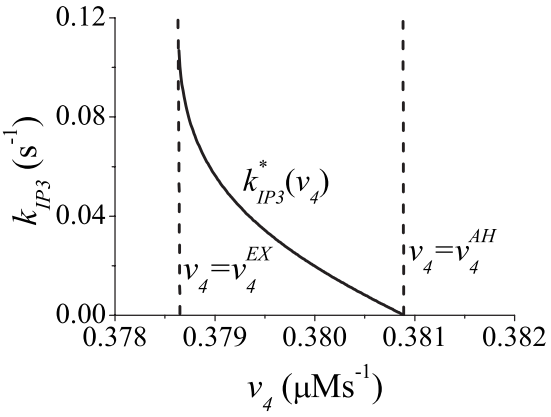

FIG. 3. The dependence of critical diffusion coefficient k_{IP_3} on the maximal rate of IP_3 production for $N=30$.

This curve is originated from the point $(v_4^{AH},0)$ corresponding to Andronov-Hopf bifurcation in the single cell. Then, the network has oscillatory dynamics in the parameter region located to the right-hand side from the line $v_4=v_4^{AH}$. Line $v_4=v_4^{ex}$ bounds the region of excitable dynamics where the network steady state is locally stable. Critical curve $k^*_{IP_3}(v_4)$ hits the line $v_4=v_4^{ex}$ in some point where the largest eigenvalue $\lambda_{max}(v_4)$ is tangent to the zero line.

Let us consider phase dynamics of the emergent oscillatory pattern. It appears that IP_3 diffusion does not provide the intercellular phase locking of the oscillations [Fig. 4(a)]. The phases computed relative to a reference periodic signal taken at the mean network frequency show an irregular pattern with phase oscillation, rotation, and reset at certain time intervals. A snapshot of the phase pattern in lattice space, $(j,k,z_{j,k})$, is shown in Fig. 4(b). In its irregular structure one can notice a "chessboard" order indicating that the neighboring cells tend to oscillate antiphase. Such a tendency can be easily explained in terms of our stability analysis (3)–(8). In

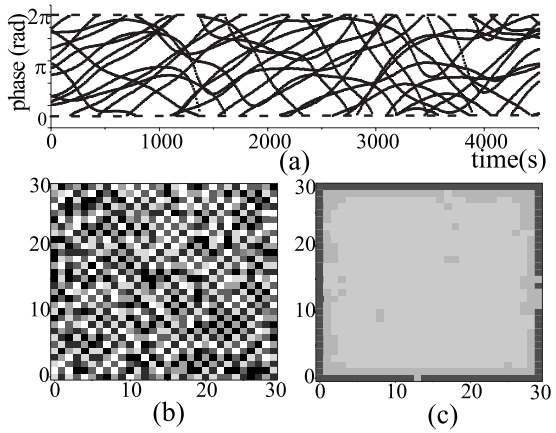

FIG. 4. (a) Superimposed traces of oscillation phases taken from the first 10 units at $k=15$. Phases evolve in a complex incoherent manner. (b) Snapshot of phase distribution in the lattice space (j,k) at $t=1000$ s. Phase values are shown by six-level gray scale of the interval $[0,2\pi]$. (c) Oscillation frequencies in the lattice space (j,k) averaged over 10^5 periods. Frequency values are shown by six-level gray scale of the interval [0.111, 0.115 Hz].

the $3N$-dimensional phase space the unstable eigenvalues define corresponding manifolds (eigenvectors) of the steady state. According to Eq. (7) the first unstable pair $(s,l=1)$ yields $S\approx 4$ for large N. It follows from (3) that the corresponding manifold satisfies the condition

$$A_{j,k} \approx -(\Delta A)_{j,k}/4, \quad j,k=1,2,\ldots,N. \tag{9}$$

Since Eqs. (9) are satisfied for arbitrary perturbations then for any directly connected cells in the network the manifold is close to perfect antiphase motions, $A_{j,k}=-A_{j\pm 1,k}$, $A_{j,k}=-A_{j,k\pm 1}$. When a number of unstable eigenmodes coexist for $k_{\mathrm{IP}_3}\geqslant k^*_{\mathrm{IP}_3}$ their manifolds with $s,l\ll N$ will be also close to (9). Accordingly, the instability signal tends to set the antiphase relations between neighboring cells [Fig. 4(b)]. In other words, the instability can only generate patterns with maximal intercellular diffusive current. This fact also agrees with previous experimental studies [11] shown that IP_3 diffusion can stabilize the antiphase calcium signals in the coupled oscillatory astrocyte cells. In contrast with the irregular phase dynamics local cell frequencies averaged over a large number of oscillation periods tend to be synchronized forming frequency clusters [Fig. 4(c)]. Note that the cluster profile resembles the lattice topology with "imperfections" along boundaries.

For increasing k_{IP_3} the amplitude of the spontaneous oscillations grow and can reach the excitation threshold. Then, calcium pulse generation becomes possible. Since the oscillations are modulated in amplitude such local excitations will appear spontaneously in time and in space. They affect the neighbors to generate calcium pulses if their oscillations have been in the appropriate phase. Thus, the intercellular signal propagation can be facilitated due to the presence of spontaneous subthreshold oscillations. This mechanism is illustrated in Fig. 5.

In summary, we have theoretically shown that diffusive coupling in astrocytes by means of IP_3 transport can be a mechanism of generating spontaneous oscillations in originally nonoscillatory cells. There are two principal features of this instability: (i) The oscillations comprise a certain number of close "eigenfrequencies" whose interaction leads to slow amplitude modulations and phase variations with no phase locking, (ii) the oscillatory signal arises as antiphase oscillations of pairs of network cells with direct coupling. The instability is a network effect of interaction of a large number of locally coupled cells. Note that due to the antiphase local synchrony it has no analogs in continuous (homogenized) reaction-diffusion systems. For example, typically in activator-inhibitor systems Andronov-Hopf bifurcation leads to homogeneous oscillations or Turing instability induced by diffusion leading to static inhomogeneous patterns. Discussing the possible importance of the spontaneous low-amplitude oscillations for astrocyte dynamics we note that they could (i) facilitate calcium signal generation and transmission by lowering the effective excitation threshold and (ii) provide a certain "timing" due to the "substrate" oscillations for the astrocyte activity patterns (Fig. 5).

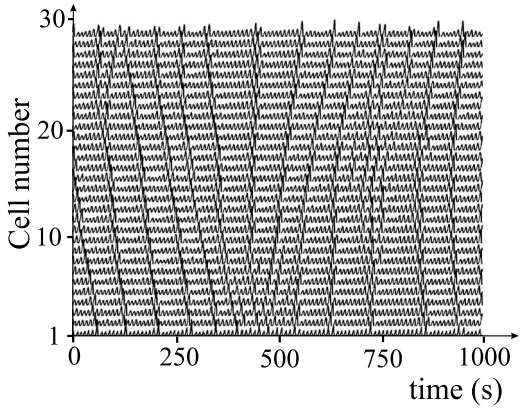

FIG. 5. Raster plot of propagating calcium pulses, $v_4=0.3805\ \mu\mathrm{M\ s^{-1}}$, $k_{\mathrm{IP}_3}=0.15\ \mathrm{s^{-1}}$, $N=30$.

ACKNOWLEDGMENTS

This work was supported by the Russian Foundation for Basic Research (Grants No. 08-02-00724 and No. 08-04-97109), by the MCB Program of Russian Academy of Science, by a grant of the President of the Russian Federation (Grant No. MD-4602.2007.2), and by the Russian Science Support Foundation.

[1] A. Verkhratsky and A. Butt, *Glial Neurobiology* (Wiley, New York, 2007).
[2] M. Falcke, Adv. Phys. **53**, 255 (2004).
[3] A. Volterra, and J. Meldolesi, Nat. Rev. Neurosci. **6**, 626 (2005).
[4] S. Nadkarni and P. Jung, Phys. Rev. Lett. **91**, 268101 (2003).
[5] V. Volman, E. Ben-Jacob, and H. Levine, Neural Comput. **19**, 303 (2007).
[6] A. N. Silchenko and P. A. Tass, Biol. Cybern. **98**, 61 (2008).
[7] A. V. Semyanov, Neurochem. Int. **52**, 31 (2008).
[8] G. W. De Young and J. Keizer, Proc. Natl. Acad. Sci. U.S.A. **89**, 9895 (1992).
[9] M. V. L. Bennett, J. E. Contreras, F. F. Bukauskas, and J. C. Saez, Trends Neurosci. **26**, 610 (2003).
[10] M. DePitta, V. Volman, H. Levine, G. Pioggia, D. DeRossi, and E. Ben-Jacob, Phys. Rev. E **77**, 030903(R) (2008).
[11] G. Ullah, P. Jung, and A. H. Cornell-Bell, Cell Calcium **39**, 197 (2006).
[12] M. R. Bennett, L. Farnell, and W. G. Gibson, Biophys. J. **89**, 2235 (2005).
[13] M. M. Halassa *et al.*, J. Neurosci. **27**, 6473 (2007).
[14] V. I. Nekorkin, and M. G. Velarde, *Synergetic Phenomena in Active Lattices* (Springer, Berlin, 2002).